energies

MDPI

Article

Energy-Neutral Operation Based on Simultaneous Wireless Information and Power Transfer for Wireless Powered Sensor Networks

Hyun-Ho Choi [1] and Jung-Ryun Lee [2,*]

[1] Department of Electrical, Electronic and Control Engineering, Hankyong National University, Anseong 17579, Korea; hhchoi@hknu.ac.kr
[2] School of the Electrical Engineering, Chung-Ang University, Seoul 06974, Korea
* Correspondence: jrlee@cau.ac.kr

Received: 21 August 2019; Accepted: 04 October 2019; Published: 10 October 2019

Abstract: For energy-neutral operation (ENO) of wireless sensor networks (WSNs), we apply a wireless powered communication network (WPCN) to a WSN with a hierarchical structure. In this hierarchical wireless powered sensor network (WPSN), sensor nodes with high harvesting energies and good link budgets have energy remaining after sending their data to the cluster head (CH), whereas the CH suffers from energy scarcity. Thus, we apply the simultaneous wireless information and power transfer (SWIPT) technique to the considered WPSN so that the sensor nodes can transfer their remaining energy to the CH while transmitting data in a cooperative manner. To maximize the achievable rate of sensing data while guaranteeing ENO, we propose a novel ENO framework, which provides a frame structure for SWIPT operation, rate improvement subject to ENO, SWIPT ratio optimization, as well as clustering and CH selection algorithm. The results of extensive simulations demonstrate that the proposed ENO based on SWIPT significantly improves the achievable rate and reduces the energy dissipated in the network while guaranteeing ENO, in comparison with the conventional schemes without SWIPT.

Keywords: energy-neutral operation; wireless powered sensor network; simultaneous wireless information and power transfer; energy harvesting; clustering

1. Introduction

With the emergence of energy harvesting (EH) techniques, sensors can be equipped with EH modules to acquire additional energy from the ambient resources (i.e., solar radiation, wind, vibrations, radio-frequency (RF) power, etc.) Such EH sensors do not break down due to energy shortages as long as the energy consumption is less than the harvested energy, so they can operate perpetually with a desired performance level, which is called energy neutral operation (ENO) [1].

According to the controllability of energy sources, ENO approaches can be classified as ambient energy harvesting (AEH) or wireless power transfer (WPT). AEH is the process of transforming any ambient resource, such as solar radiation or wind, into readily utilizable energy [2]. In AEH, it is difficult to control the amount of energy supplied due to the random nature of the employed energy sources. Thus, by predicting the energy source activity, various adaptive energy management schemes, which control the duty cycles [3], transmission power [4], sampling rates [5], and routing paths [6] of sensor nodes, have been proposed to guarantee ENO. Meanwhile, WPT uses a controllable RF power source, such as a power beacon and hybrid access point (HAP) (While a power beacon only acts as a power transmitter, a HAP acts as both a power transmitter and a communication gateway.) Various radio resources (e.g., time, bandwidth, waveform, antennas, etc.) can be controlled to transfer the RF

energy efficiently while ensuring ENO [7,8]. Such controllability at the RF power source adds a new dimension to the system optimization, and various optimization problems have been addressed to maximize system performance while ensuring ENO [9,10].

The potential of WPT has recently begun to emerge in two major applications: wireless powered communication networks (WPCNs) [11] and simultaneous wireless information and power transfer (SWIPT) [12]. A WPCN consists of a dedicated power source (e.g., HAP) and wireless devices (e.g., sensors), where the wireless devices are powered by the RF waves sent from the HAP and then transmit data to the HAP using the harvested energy. On the other hand, SWIPT is a technique that enables both wireless information transmission (WIT) and wireless energy transfer (WET) to be attained simultaneously via the same electromagnetic wave [13]. To this end, one of two mode-switching techniques, namely power splitting (PS) or time switching (TS), is used to balance the ratio of WIT to WET [14].

One of the main challenges in the operation of wireless sensor networks (WSNs) is the limited battery time of the sensor nodes. WSNs typically consist of massive numbers of sensor nodes, so it is costly and impractical to replace their batteries regularly [15]. It is also very serious that sensing errors and link failures often occur when the battery life of a sensor node is almost over. Therefore, extending the lifetimes of sensor nodes while maintaining their sensing performance is a major problem in WSNs [16,17].

To address this issue, we apply the WPT technology to a WSN. Firstly, we apply the basic WPCN concept to a hierarchical network structure, as many WSN applications use this structure to reduce the total cost of the transmission links [18]. In this wireless powered sensor network (WPSN) with a hierarchical structure, all of the nodes in the cell harvest wireless energy from the HAP, as in a WPCN. However unlike in a WPCN, the sensor nodes are clustered and transmit the sensing data to the cluster head (CH) without directly transmitting the data to the HAP. The CH gathers and aggregates all of the sensing data received from its member nodes and then transmits the aggregated data to the HAP at one time.

If all of the sensor nodes perform the same task and thus generate sensing data of the same size, the maximum rate of the sensing data collected in the WSN will be limited by the worst sensor node with low harvesting energy and poor link budget [19,20]. Thus, all of the sensor nodes only need to support the same data rate as the worst node so that some sensor nodes may have energy remaining after transmitting their sensing data to the CH. On the other hand, the CH needs more processing for the reception and aggregation of multiple sensing data and has to transmit the aggregated data to the HAP via an uplink; thus, it requires more energy in general (i.e., the CH becomes the highest energy-consuming node in the cluster with high probability). Considering this situation, we apply the SWIPT technique to the considered WPSN so that the sensor nodes could transfer their remaining energy to the CH while transmitting data in a cooperative way. This approach can increase the sensing data rate in the cluster while guaranteeing the ENO of sensor nodes because the CH receives additional energy from its member nodes and the sensor nodes give up only the remaining energy. The objective of our study is to maximize the achievable rate of sensing data while guaranteeing ENO in the considered WPSN. The main contributions can be summarized as follows:

- We design a frame structure to operate SWIPT in the hierarchical WPSN structure. The frame is divided into WET, SWIPT, and WIT slots, and each sensor node uses either a PS or TS method in the allocated SWIPT slot.
- We numerically express the achievable rate of sensing data collected in each cluster subject to the guarantee of ENO of the sensor nodes and obtain the total energy dissipated in the cluster depending on the use of SWIPT.
- We develop an algorithm that finds the optimal SWIPT ratio in terms of PS and TS to maximize the achievable rate of sensing data in the cluster.
- Finally, we design a clustering and CH selection algorithm based on the K-means clustering algorithm to maximize the achievable rate in the entire network.

The rest of this paper is organized as follows. In Section 2, we survey related previous studies and explain the originality of our study. In Section 3, we describe the considered WPSN system and introduce our basic approach. In Section 4, we explain the proposed ENO framework in terms of frame

structure, the details of ENO, the optimal SWIPT ratio, and clustering and CH selection. In Section 5, the simulation results are discussed. Finally, we present the conclusions in Section 6.

2. Related Works

In this section, we survey the previous studies on WPT-based ENO, which are directly related to the proposed approach.

2.1. WPCN

WPCN basically guarantees ENO because all of the devices in the cell use only the energy supplied by the HAP or power beacon. Thus, most studies on WPCNs have been focused on system optimization considering resource allocation [21], beamforming [22], cooperative communication [23], and full-duplex communication [24]. These topics have been investigated in a flat network structure where the wireless device directly transmits data to the HAP, while hierarchical networks like WSNs have not been considered.

A few studies have addressed hierarchical structures in WPCNs. For instance, cluster-based cooperation in a WPCN was proposed in [25], where an HAP with multiple antennas exploited energy beamforming to focus more transferred power to the CH considering the performance to be limited by the high energy consumption of the CH. Then, joint optimization of the energy beamforming design, transmit times of all of the nodes, and transmission power of the CH was performed to maximize the minimum data rate achievable among all of the nodes (i.e., max-min throughput). In [26], a WPSN consisting of one HAP, a near cluster, and the corresponding far cluster was considered and a cluster cooperation concept was proposed. If the sensors in the near cluster do not have their own information to transmit, acting as relays, they can help the sensors in the far cluster forward information to the HAP in an amplify-and-forward manner. In [27], a WPSN was divided into several layers and the exact border of each layer was obtained in order to alleviate the doubly near-far effect, and the energy broadcasted by the HAP and radius of each layer were optimized jointly. Furthermore, a multi-hop WPCN based on user-cooperative multi-hop transmission was considered in [28] to improve the throughput fairness, and the max-min throughput was optimized by resource allocation (i.e., transmission power and time). In a WPCN environment, these previous studies considered the WET from the HAP without using SWIPT technology.

2.2. SWIPT in WSN

SWIPT has been applied to WSNs in various ways to overcome their energy limitations. Numerous surveys of SWIPT in WSNs have been published recently [29–31]. For instance, [29] summarized the current research on SWIPT-based cooperative sensor networks, in which SWIPT is applied to WSNs in terms of dual-hop and multi-hop relays. Meanwhile, [30] focused on the integral aspects of SWIPT in other prominent networks, such as device-to-device networks, vehicular ad hoc networks, wireless body area networks, WSNs, and so on, and presented open issues and challenges in SWIPT application. In [31], an overview of SWIPT/WPT-enabled WSNs was provided and future directions were suggested.

Meanwhile, [32] described a WSN consisting of multiple clusters and a sink node, in which the CH of each cluster performs SWIPT to give energy to relay nodes with low energies. In [33], a SWIPT-powered sensor network was considered in which each source node operates SWIPT as both an information transmitter and an energy transferrer, and the destination node works as an information receiver while the other nodes work as energy harvesters. Furthermore, [34] focused on the deployment of a WSN and its routing strategy when SWIPT is applied to the WSN. The basic idea is to reduce the total recharging cost to enhance the lifespan of the WSN. In addition, [35] proposed a dynamic routing algorithm for a renewable WSN with SWIPT. SWIPT has been adopted in many studies to overcome the energy limitations of WSNs, but SWIPT has not yet been applied in the WPCN

environment. Furthermore, these previous studies were focused on increasing the lifetimes of WSNs rather than guaranteeing ENO.

2.3. ENO Based on WPT

ENO based on WPT has been investigated in some recent work. For example, the feasibility of an energy-neutral Internet of Things (IoT) network was studied in [36] by joint utilization of EH and WPT technologies, and design guidelines for energy-neutral wireless powered networks were presented. In [37], duty cycle operation for a self-powering dual mode SWIPT system in which a sensor node adaptively controls single-tone or multi-tone communication mode was introduced and an adaptive mode switching problem was solved to maximize the achievable rate under ENO to realize a battery-free IoT network. Meanwhile, an energy management scheme for a WPSN was proposed in [38], which maximizes the RF energy transfer efficiency while guaranteeing ENO, and the proposed energy management scheme was implemented in an actual testbed to verify its operation. In [39], an adaptive duty cycle control algorithm was proposed to prevent the energy storage of a sensor node from being depleted and its ENO was validated in a multi-antenna WPSN testbed that dynamically steered a microwave beam towards a sensor node. In addition, the energy neutral Internet of drones was conceptualized in [40] to overcome the energy limitations for continuous operation of drones and to enhance the connectivity between drones. Communication and networking architectures and protocols for drones energized by WPT were presented. Although ENO was considered in SWIPT-enabled networks or WPCNs in these works, to the best of our knowledge, ENO considering both SWIPT and WPCNs has not been investigated yet.

3. System Description

Figure 1 illustrates the considered WPSN, which includes one HAP and a number of sensor nodes in a cell. The HAP is a power source that wirelessly transfers energy to all of the sensor nodes and also acts as a sink node that collects sensing information in the cell. Only the HAP has a stable energy supply, but the sensors do not have any embedded energy source or battery. The HAP periodically broadcasts an RF wave, and all of the nodes in the cell harvest energy from this RF signal. Considering the hierarchical structure, the sensor nodes are grouped into a number of clusters and one CH is selected from among the member nodes in each cluster. Thus, all of the sensor nodes send sensing data to their CH instead of directly to the HAP. The CH aggregates all of the sensing information received from its member sensor nodes as well as its own sensing information (i.e., data fusion), then sends the aggregated data to the HAP at once.

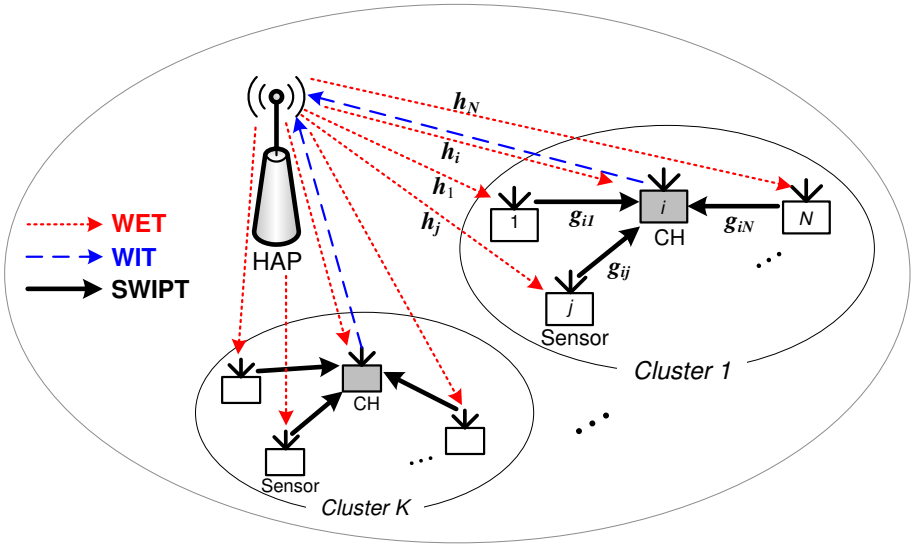

Figure 1. Considered wireless powered sensor network.

Assuming that all of the sensors perform the same sensing task, such as temperature, humidity, or fire sensing, the bit size of the sensing data transmitted by each sensor node is the same. However, the sensor nodes inherently harvest different amounts of energy depending on their distances from the HAP and consume different amounts of energy for transmission depending on their distances from the CH. Incidentally, the maximum rate of sensing data collection in the WSN is limited by the worst sensor node, which has a low harvesting energy and poor link budget [19,20]. Therefore, all of the sensor nodes only need to support the same data rate as the worst node so that some sensor nodes may have energy remaining after transmitting their sensing data to the CH. Since the CH usually requires more energy for multiple receptions, processing, and uplink transmission to the HAP, the sensor nodes transfer the remaining energy to the CH while sending their data by using the SWIPT technique, and the CH acquires additional energy while receiving data from its member nodes.

4. Proposed Energy Neutral Operation

In this section, we propose new protocols and algorithms related to the frame structure, ENO, SWIPT, clustering, and CH selection, in order to maximize the achievable rate of sensing data while guaranteeing ENO in the considered WPSN.

4.1. Frame Structure

Figure 2 shows the frame structure for the proposed ENO based on SWIPT. The frame is based on time division multiple access with time division duplexing (TDMA/TDD) and scheduling-based resource allocation is used for conflict-free transmission. Firstly, a beacon signal is broadcasted at the beginning of the frame for frame synchronization and to provide the frame configuration and scheduling information to all of the nodes in the cell. In compliance with the harvest-then-transmit protocol [21], the HAP transmits RF energy during the WET slot with length T_e. During this WET period, all of the sensor nodes harvest energy to be used in the current frame.

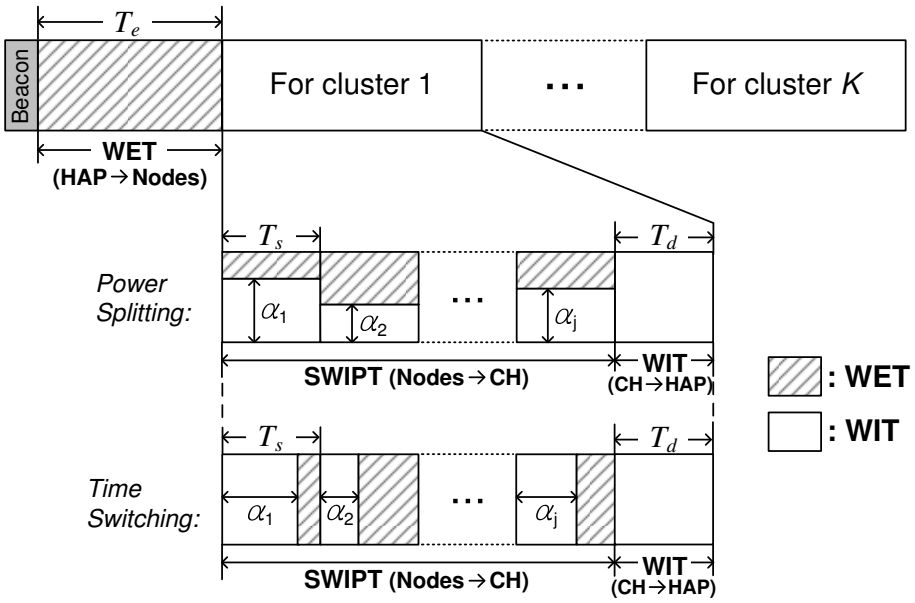

Figure 2. Frame structure for the proposed ENO based on SWIPT.

The remainder of the frame is divided and used for each cluster. The resources allocated to each cluster consist of multiple SWIPT slots for the member nodes in the cluster and one WIT slot for the CH. The total number of SWIPT slots for a certain cluster is the same as the number of member nodes in that cluster, and the length of a SWIPT slot is set to T_s. Each SWIPT slot is reserved for each sensor node through a pre-scheduling mechanism so that access collision does not occur [41]. On the other hand,

the last WIT slot is dedicated to the CH only for WIT and has a length of T_d. Hence, the total length of the frame depends on the number of clusters and the number of member nodes in each cluster.

The sensor node transmits the sensing data to its CH in the SWIPT slot allocated to itself. Simultaneously, it transfers the remaining energy (if it exists) to the CH by using SWIPT based on either the PS or TS method. Each sensor node j uses a portion α_j of power or time for WIT and the remaining portion $(1-\alpha_j)$ for WET. During these SWIPT slots, the CH sequentially receives the sensing data while receiving additional energy from its member nodes. Then, the CH aggregates all of the sensing information and transmits the aggregated sensing data to the HAP at the last WIT slot. Here, the CH uses not only the energy initially provided by the HAP but also the energy additionally received from its member nodes. It is noted that we do not consider the ambient energy harvesting between any nodes [42] because the amount of energy harvested is negligible due to the long distance between nodes and the sensor nodes may inherently stay in sleep state except for its transmit and receive periods.

4.2. Energy Neutral Operation

We explain the proposed ENO based on SWIPT in detail in this section. The proposed ENO is performed on a per-cluster basis. Without loss of generality, we can consider only one cluster assuming that the clustering and CH selection are completed in advance (The clustering and CH selection algorithm is presented in Section 4.4.). Suppose that there are N sensor nodes in the cluster. Let $\mathcal{N}$ be the set of sensor nodes in the cluster, i.e., $\mathcal{N} = \{1, 2, \cdots, N\}$. We denote the selected CH node as i, where $\exists i \in \mathcal{N}$, and denote the other sensor nodes as j, where $\forall j \in \mathcal{N} \setminus \{i\}$. For simplicity, we assume that there is channel reciprocity between any two nodes. As illustrated in Figure 1, h_j denotes the channel power gain between the HAP and any node j, and g_{ij} denotes the channel power gain from sensor node j to CH i.

The energy harvested by node j from HAP is expressed as

$$E_j^{\text{har}} = \zeta_j h_j P T_e, \ \forall j \in \mathcal{N} \tag{1}$$

where $0 < \zeta_j < 1$ is an EH efficiency of node j, and P is the constant transmission power of the HAP. The transmission power of sensor node j for transmitting data to the CH during the SWIPT slot is given by

$$P_j = \frac{\eta_j E_j^{\text{har}}}{T_s} = \frac{\eta_j \zeta_j h_j P T_e}{T_s}, \ \forall j \in \mathcal{N} \setminus \{i\} \tag{2}$$

where $0 < \eta_j < 1$ is the ratio of the energy used for only transmission except reception, processing, and circuit operations to the total energy harvested in node j. By Shannon's theorem, the achievable rate of transmission from sensor node j to the CH i is expressed as

$$R_{ij} = T_s \log_2 \left(1 + \frac{g_{ij} P_j}{\sigma^2}\right), \ \forall j \in \mathcal{N} \setminus \{i\} \ \text{(bits/Hz)} \tag{3}$$

where σ^2 is the noise power at the receiving side, and the unit of this rate has bits/Hz reflecting the transmission time T_s.

If SWIPT is not used, as in the conventional method, the CH uses only the energy harvested from the HAP. Thus, the transmission power of CH i for transmitting data to the HAP during the WIT slot is given by

$$P_i = \frac{\eta_i E_i^{\text{har}}}{T_d} = \frac{\eta_i \zeta_i h_i P T_e}{T_d}. \tag{4}$$

Then, the achievable rate of transmission from the CH i to the HAP is given by

$$R_i = T_d \log_2 \left(1 + \frac{h_i P_i}{\sigma^2}\right) \text{ (bits/Hz)}. \tag{5}$$

The maximum rate of sensing data that can be collected in this cluster is limited by the minimum rate of the transmission links [19,20]. Therefore, when SWIPT is not used, the achievable rate of sensing data in this cluster is determined by

$$R^{\text{noSwipt}} = \min \left[\min_{j \in \mathcal{N} \setminus \{i\}} \left\{ R_{ij} \right\}, R_i \right]. \tag{6}$$

Because the achievable rate of sensing data is determined by the minimum rate of the transmission links, the sensor nodes with higher R_{ij} can consume only the energy required to satisfy this minimum rate and then transmit the remaining energy to the CH using the SWIPT technique. When PS-based SWIPT is applied, node j uses power $\alpha_j P_j$ for WIT and the remaining power $(1-\alpha_j)P_j$ for WET. Thus, the achievable rate of transmission from sensor node j to CH i is expressed as

$$\begin{aligned} R_{ij}^{\text{PS}} &= T_s \log_2 \left(1 + \tfrac{g_{ij}\alpha_j P_j}{\sigma^2}\right) \\ &= T_s \log_2 \left(1 + \tfrac{\eta_j \zeta_j g_{ij} h_j \alpha_j P T_e}{\sigma^2 T_s}\right), \ \forall j \in \mathcal{N} \setminus \{i\} \text{ (bits/Hz)}. \end{aligned} \tag{7}$$

On the other hand, when TS-based SWIPT is applied, node j uses time $\alpha_j T_s$ for WIT and the remaining time $(1-\alpha_j)T_s$ for WET. Hence, the achievable rate of transmission from sensor node j to CH i is expressed as

$$\begin{aligned} R_{ij}^{\text{TS}} &= \alpha_j T_s \log_2 \left(1 + \tfrac{g_{ij} P_j}{\sigma^2}\right) \\ &= \alpha_j T_s \log_2 \left(1 + \tfrac{\eta_j \zeta_j g_{ij} h_j P T_e}{\sigma^2 T_s}\right), \ \forall j \in \mathcal{N} \setminus \{i\} \text{ (bits/Hz)}. \end{aligned} \tag{8}$$

In both the PS and TS methods, the amount of energy that CH i additionally obtains is given by

$$E_i^{\text{add}} = \sum_{j \in \mathcal{N} \setminus \{i\}} \zeta_i g_{ij} (1-\alpha_j) P_j T_s. \tag{9}$$

Then, when SWIPT is used, the transmission power of CH i is updated as

$$P_i^{\text{swipt}} = \frac{\eta_i (E_i^{\text{har}} + E_i^{\text{add}})}{T_d}. \tag{10}$$

Moreover, the achievable rate of transmission from CH i to the HAP is represented as

$$\begin{aligned} R_i^{\text{swipt}} &= T_d \log_2 \left(1 + \tfrac{h_i P_i^{\text{swipt}}}{\sigma^2}\right) \\ &= T_d \log_2 \left\{1 + \tfrac{\eta_i h_i (E_i^{\text{har}} + E_i^{\text{add}})}{\sigma^2 T_d}\right\} \\ &= T_d \log_2 \left\{1 + \tfrac{\eta_i \zeta_i h_i P T_e \left(h_i + \sum_{j \in \mathcal{N} \setminus \{i\}} \eta_j \zeta_j (1-\alpha_j) g_{ij} h_j\right)}{\sigma^2 T_d}\right\} \text{ (bits/Hz)}. \end{aligned} \tag{11}$$

Finally, the achievable rates of sensing data when SWIPT is used according to PS and TS are respectively expressed as

$$R^{\text{swipt}} = \begin{cases} \min \left[\min_{j \in \mathcal{N} \setminus \{i\}} \left\{ R_{ij}^{\text{PS}} \right\}, R_i^{\text{swipt}} \right], & \text{if PS is used} \\ \min \left[\min_{j \in \mathcal{N} \setminus \{i\}} \left\{ R_{ij}^{\text{TS}} \right\}, R_i^{\text{swipt}} \right], & \text{if TS is used.} \end{cases} \tag{12}$$

In WSNs, energy dissipation can occur because the sensor node does not need to consume more energy than the energy required to attain the achievable rate of sensing data. This metric is important for measuring the energy efficiency in WSNs [43]. The amount of energy dissipated in the sensor node is defined as the difference between the energy harvested and the energy required to satisfy the achievable rate. In the case without using SWIPT, all of the nodes only need to satisfy R^{noSwipt} given as Equation (6). Thus, the amounts of energy dissipated in sensor node j and CH i are respectively calculated as

$$\mathcal{E}_j^{\text{noSwipt}} = \left\{ P_j - \frac{\sigma^2}{g_{ij}} \left(2^{\frac{R^{\text{noSwipt}}}{T_s}} - 1 \right) \right\} T_s, \ \forall j \in \mathcal{N} \setminus \{i\} \tag{13}$$

$$\mathcal{E}_i^{\text{noSwipt}} = \left\{ P_i - \frac{\sigma^2}{h_i} \left(2^{\frac{R^{\text{noSwipt}}}{T_d}} - 1 \right) \right\} T_d. \tag{14}$$

Therefore, the total amount of energy dissipated in the cluster is expressed as

$$\mathcal{E}^{\text{noSwipt}} = \mathcal{E}_i^{\text{noSwipt}} + \sum_{j \in \mathcal{N} \setminus \{i\}} \mathcal{E}_j^{\text{noSwipt}}. \tag{15}$$

On the other hand, when SWIPT is used, all of the nodes only need to satisfy R^{PS} or R^{TS} depending on the SWIPT method used. However, SWIPT is not necessary if $R_i \geq \min_j \{R_{ij}\}$ because the rate of the CH is sufficiently high that the CH does not need to receive energy from its member nodes. In this case, the energy dissipated in the cluster is the same as Equation (15). However, in the opposite case, i.e., if $R_i < \min_j \{R_{ij}\}$, the energy dissipated in sensor node j is zero because it transfers all of the remaining energy to the CH. Thus, the energy dissipated in sensor node j is given by

$$\mathcal{E}_j^{\text{swipt}} = \begin{cases} 0, & \text{if } R_i < \min_j \{R_{ij}\} \\ \mathcal{E}_j^{\text{noSwipt}}, & \text{otherwise.} \end{cases} \tag{16}$$

Moreover, the energy dissipated in CH i is obtained as

$$\mathcal{E}_i^{\text{swipt}} = \left\{ P_i^{\text{swipt}} - \frac{\sigma^2}{h_i} \left(2^{\frac{R^{\text{swipt}}}{T_d}} - 1 \right) \right\} T_d. \tag{17}$$

Finally, when SWIPT is used, the total amount of energy dissipated in the cluster is expressed as

$$\mathcal{E}^{\text{swipt}} = \mathcal{E}_i^{\text{swipt}} + \sum_{j \in \mathcal{N} \setminus \{i\}} \mathcal{E}_j^{\text{swipt}}. \tag{18}$$

Note that it is always true that $\mathcal{E}_j^{\text{swipt}} \geq 0$ and $\mathcal{E}_i^{\text{swipt}} \geq 0$ since $R^{\text{swipt}} \leq R_i^{\text{swipt}}$, so the ENO of all of the nodes is guaranteed.

4.3. Optimal SWIPT Ratio

For a given CH i, the optimal SWIPT ratio that maximizes R^{swipt} is formulated as

$$\begin{aligned} \overrightarrow{\alpha}^* &= \arg\max_{\overrightarrow{\alpha}} R^{\text{swipt}} \\ &= \arg\max_{\overrightarrow{\alpha}} \min \left[\min_{j \in \mathcal{N} \setminus \{i\}} \left\{ R_{ij}^{\text{swipt}} \right\}, R_i^{\text{swipt}} \right] \end{aligned} \tag{19}$$

where $\overrightarrow{\alpha} = \{\alpha_j\}, \forall j \in \mathcal{N} \setminus \{i\}$, and $R_{ij}^{\text{swipt}} = R_{ij}^{\text{PS}}$ or R_{ij}^{TS} according to the SWIPT method used. From Equations (7), (8), and (11), as $\overrightarrow{\alpha}$ increases, R_{ij}^{swipt} increases but R_i^{swipt} decreases, and vice versa. Thus, there is a tradeoff between $\min_j \left\{ R_{ij}^{\text{swipt}} \right\}$ and R_i^{swipt} according to $\overrightarrow{\alpha}$. In this case, the optimal

solution of the given max-min problem is found when $\min_j \left\{R_{ij}^{\text{swipt}}\right\} = R_i^{\text{swipt}}$ [44]. To find the optimal $\overrightarrow{\alpha}^*$ that satisfies $\min_j \left\{R_{ij}^{\text{swipt}}\right\} = R_i^{\text{swipt}}$, we design an iterative algorithm, as shown in Algorithm 1. Since SWIPT is performed when $\min_j \{R_{ij}\} > R_i$, we set the initial target rate R_i^{tar} to $\min_j \{R_{ij}\}$ and adjust the target rate to make all of the link rates equal. In every step, α_j is determined to satisfy R_i^{tar} according to the PS or TS method. The computational complexity of the proposed SWIPT algorithm is given by $O(L|\mathcal{N}|)$ where L is the number of iterations for the first loop and $|\mathcal{N}|$ is the number of nodes in cluster.

Algorithm 1: SWIPT algorithm

Ensure: i is CH and $j \in \mathcal{N} \setminus \{i\}$
1: Initialize $R_i^{\text{tar}} \leftarrow \min_j\{R_{ij}\}$
2: **repeat**
3: **if** *PS is used* **then**
4: $\alpha_j \leftarrow \left(2^{R_i^{\text{tar}}/T_s} - 1\right) \frac{\sigma^2 T_s}{\eta_j \zeta_j g_{ij} h_j P T_e}$ from Equation (7)
5: **else if** *TS is used* **then**
6: $\alpha_j \leftarrow \frac{R_i^{\text{tar}}}{T_s \log_2\left(1+\frac{\eta_j \zeta_j g_{ij} h_j P T_e}{\sigma^2 T_s}\right)}$ from Equation (8)
7: **end if**
8: Update E_i^{add} according to Equation (9)
9: Update R_i^{swipt} according to Equation (11)
10: $R_i^{\text{tar}} \leftarrow \frac{R_i^{\text{swipt}}+R_i^{\text{tar}}}{2}$
11: **until** $R_i^{\text{swipt}} \geq R_i^{\text{tar}}$
12: Return $\alpha_j, \forall j \in \mathcal{N} \setminus \{i\}$

4.4. Clustering and CH Selection

Next, we discuss how to form appropriate clusters and select the optimal CH. The proposed clustering and CH selection algorithm is described in Algorithm 2. When the number of clusters is K, let $\mathcal{N}_k$ be the set of nodes in cluster $k \in \{1, 2, \cdots, K\}$. Without loss of generality, we denote i_k as the CH in cluster k, where $\exists i_k \in \mathcal{N}_k$, and j_k as a sensor node in the cluster k, where $\forall j_k \in \mathcal{N}_k \setminus \{i_k\}$. The proposed algorithm is based on the well-known K-means clustering algorithm [45]. Thus, the initial K clusters are determined using the K-means algorithm, and the initial CH in each cluster is determined to be the node closest to the centroid of each cluster. Consequently, the initial cluster and CH are determined by only the distance among sensor nodes without considering the distance between the sensor node and the HAP. However, this distance directly affects the amount of energy harvested, so it is necessary to modify the basic process of the K-means algorithm to make it suitable for the proposed ENO scheme.

The proposed algorithm mainly consists of two parts, similarly to the K-means algorithm. Firstly, each node reselects the best cluster among the predetermined clusters. After calculating $R_{i_k j}$ and R_{i_k} for each CH i_k, node j selects the cluster that provides the highest $R_{i_k j}$ among the clusters satisfying $R_{i_k j} > R_{i_k}$. This step is included so that SWIPT can be performed without decreasing the rate of the predetermined clusters. Thereafter, the best CH is reselected in each cluster. For all nodes in each cluster $\forall i_k \in \{\mathcal{N}_k\}$, the rate of cluster k, R_k^{swipt}, is calculated using Equation (12). Then, the best CH, i_k^*, is determined as

$$\begin{aligned} i_k^* &= \arg\max_{i_k} R_k^{\text{swipt}} \\ &= \arg\max_{i_k} \min\left[\min_{j_k \in \mathcal{N}_k \setminus \{i_k\}} \left\{R_{i_k j_k}^{\text{swipt}}\right\}, R_{i_k}^{\text{swipt}}\right] \end{aligned} \tag{20}$$

where i_k^* can be found by exhaustive searching with a complexity of $O(|\mathcal{N}_k|)$. This clustering and CH selection algorithm is repeated until all of the cluster sets and CHs are no longer changed. The computational complexity of this algorithm is given by $O(N^2)$ because it is based on k-means algorithm, which has a time complexity of $O(n^2)$ where n is the input data size [45].

Algorithm 2: Clustering and CH selection

Ensure: $\mathcal{N}_k$ is the set of nodes in cluster $k \in \{1, 2, \cdots, K\}$

i_k is the CH in the cluster k, $\exists i_k \in \mathcal{N}_k$

j_k is a sensor node in the cluster k, $\forall j_k \in \mathcal{N}_k \setminus \{i_k\}$

Initialize $\mathcal{N}_k$ and $i_k \leftarrow$ K-means algorithm [45]
repeat
  /* Select the best cluster in the network */
  for *each node* $j \in \{\mathcal{N}_1 \cup \cdots \cup \mathcal{N}_K\}$ **do**
    for *each CH* i_k **do**
      Determine $R_{i_k j}$ from Equation (3)
      Determine R_{i_k} from Equation (5)
    end for
    if $\exists i_k \in \{i_k | R_{i_k j} > R_{i_k}\} \neq \emptyset$ **then**
      j's cluster $\leftarrow \arg_k \max\{R_{i_k j}\}$ for $\exists i_k \in \{i_k | R_{i_k j} > R_{i_k}\}$
    else
      j's cluster $\leftarrow \arg_k \max\{R_{i_k j}\}$ for $\forall i_k$
    end if
  end for
  /* Select the best CH in each cluster */
  for *each cluster* k **do**
    for *each node* $i_k \in \{\mathcal{N}_k\}$ **do**
      Calculate R_k^{swipt} from Equation (12)
    end for
    CH $i_k^* \leftarrow \arg_{i_k} \max\{R_k^{\text{swipt}}\}$ from Equation (20)
  end for
until $\forall \mathcal{N}_k$ *and* $\forall i_k$ *are no longer changed*

5. Results and Discussion

Table 1 summarizes the parameters used in the simulation. We evaluated the performance by adjusting the number of nodes in the network, number of clusters, and network size in appropriate ranges. We consider a square network area in an indoor environment, place the HAP at the center of the area, and randomly distribute the sensor nodes. Assuming all of the sensor nodes to be homogeneous, their EH efficiencies (ζ) are all equal to 0.8 [21]. The ratio of energy used for transmission (η) is set to 0.9 for the sensor nodes and 0.7 for the CH. For ease of exposition, we consider a simple distance-dependent path loss model given by $h_i = G d_i^{-\gamma}$ and $g_{ij} = G d_{ij}^{-\gamma}$ assuming the channel fading effect to be averaged out over the frame and all of the channels to be reciprocal [22–24]. Here, d_i is the distance between the HAP and CH i, d_{ij} is the distance between nodes i and j, G refers to the average power attenuation at a reference distance of 1 m and is set to -30 dB, and γ is the path loss exponent, which is set to 2.5 [46]. Moreover, we set the length of the WET slot (T_e) to 5 s and set the lengths of the SWIPT slot (T_s) and WIT slot (T_d) both equal to 0.1 s, assuming the aggregated sensing data to have the same size as the individual sensing data through proper data fusion [47].

Table 1. Parameter Setup.

Parameter	Value
Number of sensor nodes in WPSN	N = 100∼500 (default = 300)
Number of clusters	K = 2∼20 (default = 10)
Width of the square network	W = 10∼50 m (default = 30 m)
Transmission power of HAP	P = 46 dBm
EH efficiency	$\zeta_j = 0.8, \forall j \in \mathcal{N}$
Ratio of energy used for transmission in sensors	$\eta_j = 0.9, \forall j \in \mathcal{N} \setminus \{i\}$
Ratio of energy used for transmission in CH	$\eta_i = 0.7$
Noise spectral density	−174 dBm/Hz
Noise figure	9 dB
Channel bandwidth	1 MHz
Channel power gains	$h_i = Gd_i^{-\gamma}, g_{ij} = Gd_{ij}^{-\gamma}$
Power attenuation at a reference distance of 1 m	$G = -30$ dB
Path loss exponent	$\gamma = 2.5$
Length of WET slot	T_e = 5 s
Length of SWIPT slot	T_s = 0.1 s
Length of WIT slot	T_d = 0.1 s
Number of simulation trials	1000

For performance comparison, we consider the following five schemes:

1. *LEACH*: The CH is chosen randomly based on the stochastic threshold algorithm of the LEACH protocol [41]. The other sensor nodes are connected to the nearest CH and do not use SWIPT.
2. *K-means*: The clusters are created using the K-means clustering algorithm, and the CH is chosen as the node closest to the centroid of each cluster. SWIPT is not used.
3. *Non-SWIPT*: The clusters are created using the K-means clustering algorithm, but the CH is chosen as the node that maximize R^{noSwipt} given by Equation (6). This scheme is the baseline for checking only the effect of the WPSN without SWIPT. The performance of this scheme is given by Equations (6) and (15).
4. *ENO with PS*: The proposed clustering and CH selection algorithm is used, and PS-based SWIPT is applied. The performance is given by Equations (12) and (18).
5. *ENO with TS*: This scheme is the same as ENO with PS, except that TS-based SWIPT is applied.

Figure 3 presents the clustering results of an example case when 300 sensor nodes are deployed randomly and grouped into five clusters in a square network with a width of 30 m. Note that the LEACH protocol is omitted because the CH is randomly selected and continuously changed in LEACH. The size of each node point represents the amount of energy dissipated in the sensor node. The smaller the dot, the less energy is wasted. The results of the K-means algorithm show that the five clusters are geographically well divided. However, there is dissipated energy in most of the nodes because the K-means algorithm does not use SWIPT. Since the non-SWIPT scheme uses the K-means algorithm for clustering, the cluster set is the same, but the selected CH is different. This behavior occurs because the non-SWIPT scheme considers R_i, as shown in Equation (6), and eventually selects the CH that provides a higher rate. In this non-SWIPT case, most of the nodes have the dissipated energy distributions similar to those in the K-means algorithm because SWIPT is not used too. Figure 3c,d show the proposed SWIPT-based ENO schemes. There is no significant difference between the PS and TS methods. It is evident that the clustering results obtained using the proposed schemes are different from those generated using the K-means and non-SWIPT schemes. In addition, there is little energy dissipation at the nodes in the clusters other than Cluster 1 in the lower left corner. This is because each node transfers its remaining energy to the CH through SWIPT and the CH uses it to transmit its data. Meanwhile, SWIPT is not used in Cluster 1 because the rate of the CH is higher than the rates of the other sensor nodes (i.e., $R_i > \min_j\{R_{ij}\}$), so Cluster 1 has a dissipated energy distribution similar to that in the non-SWIPT scheme.

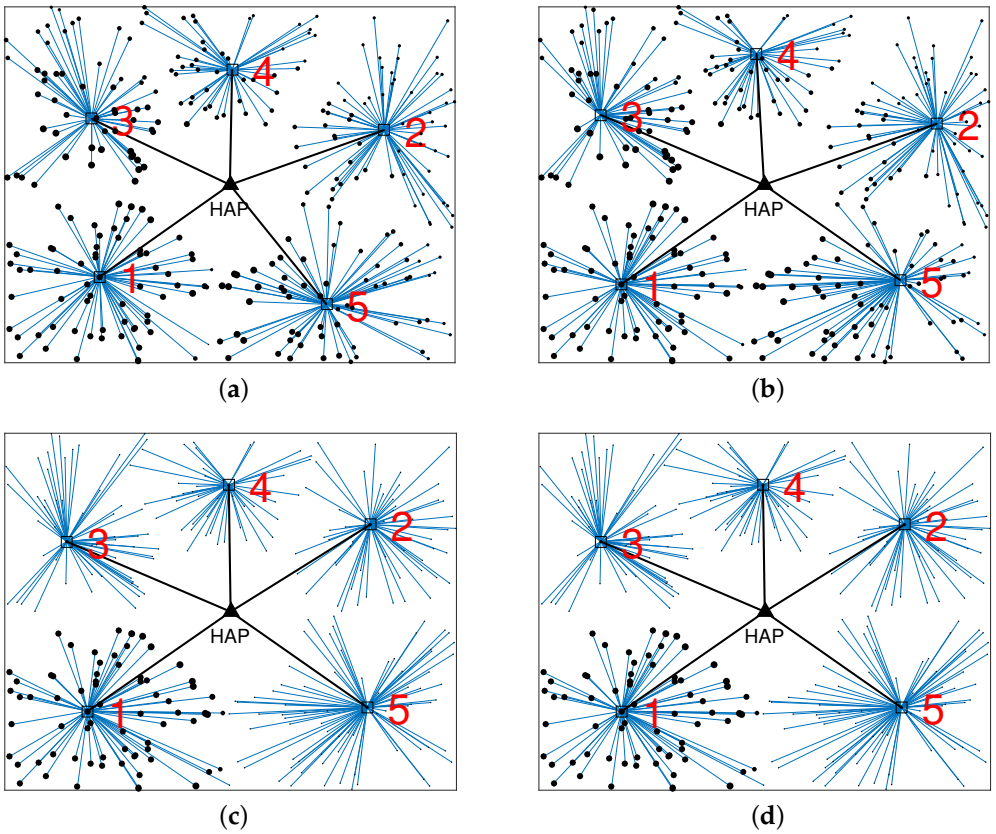

Figure 3. Clustering results of an example case when N = 300, K = 5, and W = 30 m: (**a**) K-means, (**b**) non-SWIPT, (**c**) ENO with PS, and (**d**) ENO with TS.

Figure 4 depicts the achievable rate and energy dissipated in each cluster of Figure 3. In the case of LEACH, both the achievable rate and energy dissipated are the worst because the CH is selected randomly without considering each link rates (i.e., R_{ij} and R_i). In the K-means case, the performance is improved because R_{ij} is considered for clustering and CH selection. In the non-SWIPT case, the performances are better than in the K-means case because R_i is additionally considered for CH selection. In the case of the proposed ENO with PS/TS, the achievable rate is improved more than in the non-SWIPT case because SWIPT is performed while considering both R_{ij} and R_i, and the energy dissipated in each cluster is close to zero except in Cluster 1. This result occurs because each sensor node in the cluster transfers the remaining energy to the CH using SWIPT. This energy is used by the CH to increase the achievable rate of the cluster.

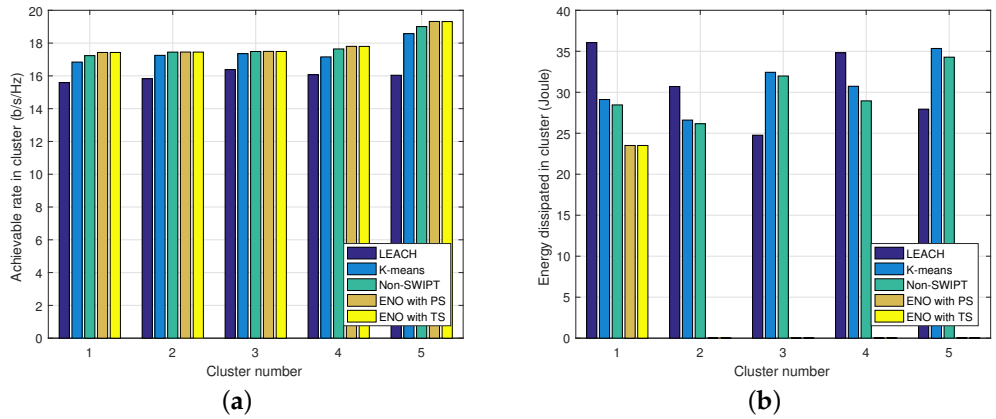

Figure 4. (**a**) Achievable rate and (**b**) energy dissipated in each cluster.

Figure 5 shows the average achievable rate in cluster and the total energy dissipated in network versus the number of clusters (K) when the number of nodes in network (N) is 300 and the width of the square network (W) is 30 m. As K increases, the achievable rate increases in all schemes. These increases occur because the distance between nodes decreases on average as K increases. The LEACH, K-means, and non-SWIPT schemes show better achievable rates in that order. The proposed ENO with PS and ENO with TS have similar performances and outperform the other conventional schemes. Moreover, as K increases, the amount of energy dissipated decreases in all schemes, because the average distance between nodes decreases and the variance of link rates becomes smaller as K increases. The three conventional schemes have similar dissipated energy, which is greater than that in the two proposed ENO schemes.

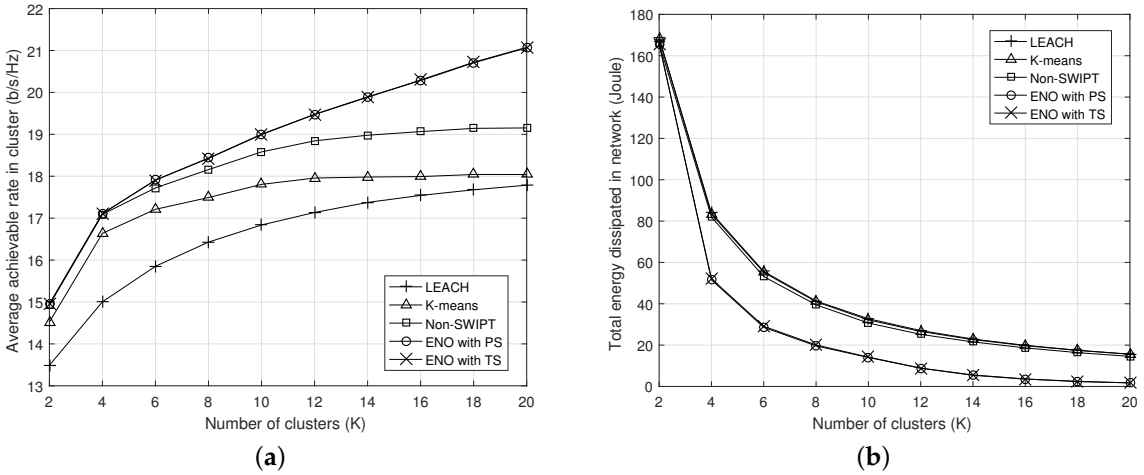

Figure 5. (**a**) Average achievable rate in cluster and (**b**) total energy dissipated in network vs. number of clusters (K) when N = 300 and W = 30 m.

Figure 6 shows the average achievable rate in cluster and the total energy dissipated in network versus the number of nodes in network (N) when K = 10 and W = 30 m. As N increases, the average achievable rate in cluster does not change much. This lack of variation occurs because the minimum rate that determines the rate of the cluster does not change significantly even if N increases. Likewise, the achievable rate improves in the order of LEACH, K-means, and non-SWIPT, and the proposed ENO with PS and TS shows the best performance. On the other hand, as N increases, the total energy dissipated increases, because the total energy dissipated is linearly proportional to N. Nevertheless, the two proposed ENO schemes show significantly lower dissipated energy levels.

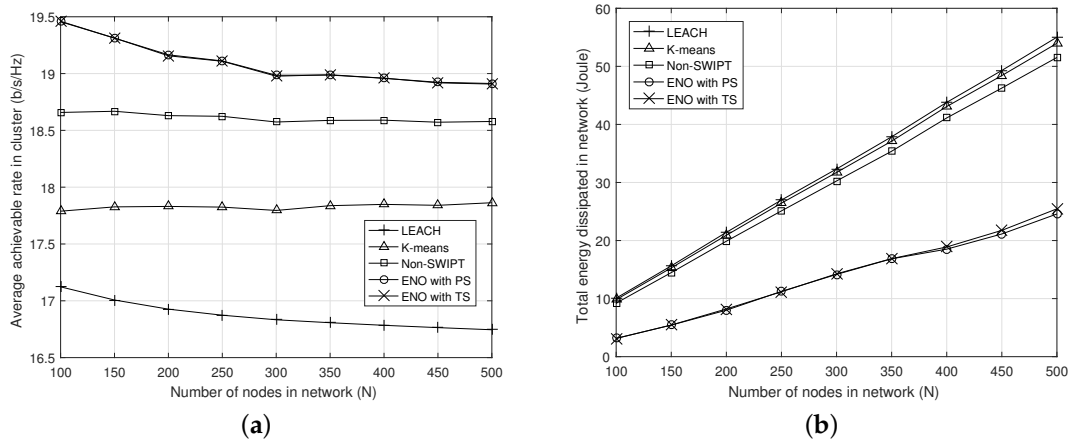

Figure 6. (**a**) Average achievable rate in cluster and (**b**) total energy dissipated in network vs. number of nodes in network (N) when K = 10 and W = 30 m.

Figure 7 shows the average achievable rate in cluster and the total energy dissipated in network versus the width of the square network (W) when N = 300 and K = 10. As the network area increases, the average achievable rate decreases because the average distance between nodes increases. On the other hand, the total energy dissipation decreases as the network area increases because the amount of energy harvested in all of the nodes becomes smaller. Likewise, the proposed ENO schemes show better performances than the conventional schemes according to the change in network size.

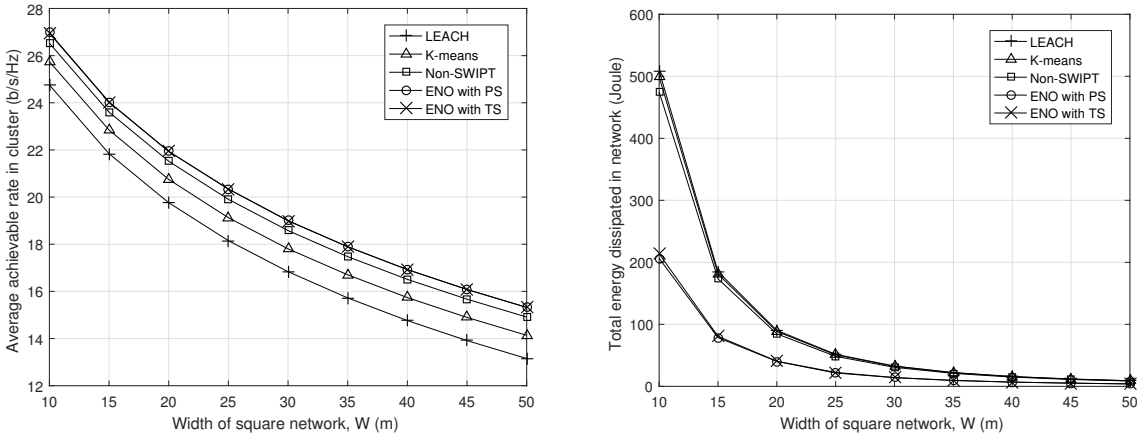

Figure 7. (**a**) Average achievable rate in cluster and (**b**) total energy dissipated in network vs. width in square network (W) when N = 300 and K = 10.

6. Conclusions

In this study, we proposed a novel ENO framework based on SWIPT in a hierarchical WPSN environment. To maximize the achievable rate of sensing data while guaranteeing ENO, new protocols and algorithms related to the frame structure, ENO, SWIPT ratios, clustering, and CH selection were presented. The simulation results showed that the proposed scheme using SWIPT performs much better in terms of the achievable rate and dissipated energy than the conventional schemes, which do not use SWIPT. It is also evident that the effect of SWIPT is greater when the number of clusters is large and the density of nodes is high. Therefore, we expect that the proposed SWIPT-based ENO can be applied to future WSNs using WPT technologies. In further research, we will investigate the distributed operations of the proposed algorithms and apply other multiple access protocols [48] considering access collision instead of the conflict-free TDMA protocol for more practical operation.

Author Contributions: H.-H.C. contributed to propose the main idea, derive the simulation results, and write most of the paper. J.-R.L. was responsible for mathematical development, verification, and proofreading of the paper.

Funding: This work was supported by the National Research Foundation of Korea (NRF) grants funded by the Korea government (MSIT) (No. 2019R1A2C4070466 and NRF-2019R1F1A1058587).

Acknowledgments: The authors are grateful to the anonymous reviewers for their comments and valuable suggestions.

Conflicts of Interest: The authors declare no conflict of interest.

References

1. Kansal, A.; Hsu, J.; Zahedi, S.; Srivastava, M.B. Power management in energy harvesting sensor networks. *ACM Trans. Embeded Comput. Syst.* **2007**, *6*, 32. [CrossRef]
2. Akan, O.B.; Cetinkaya, O.; Koca, C.; Ozger, M; Internet of hybrid energy harvesting things. *IEEE Internet Things J.* **2017**, *5*, 736–746. [CrossRef]

3. Vigorito, C.M.; Ganesan, D.; Barto, A.G; Adaptive control of duty cycling in energy-harvesting wireless sensor networks. In Proceedings of the 2007 4th Annual IEEE Communications Society Conference on Sensor, Mesh and Ad Hoc Communications and Networks, San Diego, CA, USA, 18–21 June 2007; pp. 21–30.
4. Moser, C.; Thiele, L.; Brunelli, D.; Benini, L. Adaptive power management in energy harvesting systems. In Proceedings of the 2007 Design, Automation & Test in Europe Conference & Exhibition, Nice, France, 16–20 April 2007.
5. Alippi, C.; Anastasi, G.; Di Francesco, M.; Roveri, M. Energy management in wireless sensor networks with energy-hungry sensors. *IEEE Instrum. Meas. Mag.* **2009**, *12*, 16–23. [CrossRef]
6. Eu, Z.A.; Tan, H.P.; Seah, W.K. Opportunistic routing in wireless sensor networks powered by ambient energy harvesting. *Comput. Netw.* **2010**, *54*, 2943–2966. [CrossRef]
7. Nguyen, M.T.; Nguyen, T.H. Wireless Power Transfer: A survey of techniques, and applications on communication networks. *ICSES Trans. Comput. Netw. Commun.* **2018**, *4*, 1–5.
8. Yang, G.; Yuan, D.; Liang, Y.C.; Zhang, R.; Leung, V.C. Optimal resource allocation in full-duplex ambient backscatter communication networks for wireless-powered IoT. *IEEE Internet Things J.* **2018**, *6*, 2612–2625. [CrossRef]
9. Bi, S.; Ho, C.K.; Zhang, R. Wireless powered communication: Opportunities and challenges. *IEEE Commun. Mag.* **2015**, *53*, 117–125. [CrossRef]
10. Sun, Q.; Dai, H.N.; Wang, Q.; Li, X.; Wang, H. When friendly jamming meets wireless energy transfer. In Proceedings of the 2018 IEEE International Conference on Internet of Things (iThings) and IEEE Green Computing and Communications (GreenCom) and IEEE Cyber, Physical and Social Computing (CPSCom) and IEEE Smart Data (SmartData), Halifax, NS, Canada, 30 July–3 August 2018; pp. 320–325.
11. Bi, S.; Zeng, Y.; Zhang, R. Wireless powered communication networks: An overview. *IEEE Wirel. Commun.* **2016**, *23*, 10–18. [CrossRef]
12. Lu, X.; Wang, P.; Niyato, D.; Kim, D.I.; Han, Z. Wireless charging technologies: Fundamentals, standards, and network applications. *IEEE Commun. Surv. Tutor.* **2015**, *18*, 1413–1452. [CrossRef]
13. Liu, Y.; Ding, Z.; Elkashlan, M.; Poor, H.V. Cooperative non-orthogonal multiple access with simultaneous wireless information and power transfer. *IEEE J. Sel. Commun.* **2016**, *34*, 938–953. [CrossRef]
14. Liu, L.; Zhang, R.; Chua, K.C. Wireless information and power transfer: A dynamic power splitting approach. *IEEE Trans. Commun.* **2013**, *61*, 3990–4001. [CrossRef]
15. Sudevalayam, S.; Kulkarni, P. Energy harvesting sensor nodes: Survey and implications. *IEEE Commun. Surv. Tutor.* **2010**, *13*, 443–461. [CrossRef]
16. Yick, J.; Mukherjee, B.; Ghosal D. Wireless sensor network survey. *Comput. Netw.* **2008**, *52*, 2292–2330. [CrossRef]
17. Wang, Q.; Dai, H.N.; Zheng, Z.; Imran, M.; Vasilakos, A. On connectivity of wireless sensor networks with directional antennas. *Sensors* **2017**, *17*, 134. [CrossRef] [PubMed]
18. Singh, S.K.; Singh, M.P.; Singh, D.K. A survey of energy-efficient hierarchical cluster-based routing in wireless sensor networks. *Int. J. Adv. Netw. Appl.* **2010**, *2*, 570–580.
19. Krishnamachari, B.; Estrin, D.; Wicker, S. Modelling data-centric routing in wireless sensor networks. In *IEEE Infocom*; IEEE: New York, NY, USA, 2002; Volume 2, pp. 39–44.
20. Choi, H.H. Construction of energy-efficient data aggregation tree in wireless sensor networks. *J. Korea Inf. Commun. Soc.* **2016**, *41*, 1057–1059. [CrossRef]
21. Ju, H.; Zhang, R. Throughput maximization in wireless powered communication networks. *IEEE Trans. Wireless Commun.* **2013**, *13*, 418–428. [CrossRef]
22. Liu, L.; Zhang, R.; Chua, K.C. Multi-antenna wireless powered communication with energy beamforming. *IEEE Trans. Commun.* **2014**, *62*, 4349–4361. [CrossRef]
23. Chen, H.; Li, Y.; Rebelatto, J.L.; Uchoa-Filho, B.F.; Vucetic, B. Harvest-then-cooperate: Wireless-powered cooperative communications. *IEEE Trans. Signal Process.* **2015**, *63*, 1700–1711. [CrossRef]
24. Kang, X.; Ho, C.K.; Sun, S. Full-duplex wireless-powered communication network with energy causality. *IEEE Trans. Wirel. Commun.* **2015**, *14*, 5539–5551. [CrossRef]
25. Yuan, L.; Bi, S.; Zhang, S.; Lin, X.; Wang, H. Multi-antenna enabled cluster-based cooperation in wireless powered communication networks. *IEEE Access* **2017**, *5*, 13941–13950. [CrossRef]
26. Zhang, C.; Zhang, P.; Zhang, W. Cluster cooperation in wireless-powered sensor networks: Modeling and Performance Analysis. *Sensors* **2017**, *17*, 2215. [CrossRef] [PubMed]

27. Yang, Y.; Han, Z.; Ma, G.; Gong, Y.; Qian, L. An energy-efficient hierarchical protocol for wireless powered sensor networks. In Proceedings of the 2018 IEEE 23rd International Conference on Digital Signal Processing (DSP), Shanghai, China, 19–21 November 2018.
28. Lei, M.; Zhang, X.; Ding, H.; Yu, B. Fairness-aware resource allocation in multi-Hop wireless powered communication networks with user cooperation. *Sensors* **2018**, *18*, 1890. [CrossRef] [PubMed]
29. Asiedu, D.K.P.; Shin, S.; Koumadi, K.M.; Lee, K.J. Review of simultaneous wireless information and power transfer in wireless sensor networks. *J. Inf. Commun. Converg. Eng.* **2019**, *17*, 105–116.
30. Hossain, M.A.; Noor, R.M.; Yau, K.L.A.; Ahmedy, I.; Anjum, S.S. Survey on simultaneous wireless information and power transfer with cooperative relay and future challenges. *IEEE Access* **2019**, *7*, 19166–19198. [CrossRef]
31. Perera, T.D.P.; Jayakody, D.N.K.; Sharma, S.K.; Chatzinotas, S.; Li, J. Simultaneous wireless information and power transfer (SWIPT): Recent advances and future challenges. *IEEE Commun. Surv. Tutor.* **2017**, *20*, 264–302. [CrossRef]
32. Guo, S.; Wang, F.; Yang, Y.; Xiao, B. Energy-efficient cooperative tfor simultaneous wireless information and power transfer in clustered wireless sensor networks. *IEEE Trans. Commun.* **2015**, *63*, 4405–4417. [CrossRef]
33. Liu, T.; Wang, X.; Zheng, L. A cooperative SWIPT scheme for wirelessly powered sensor networks. *IEEE Trans. Commun.* **2017**, *65*, 2740–2752. [CrossRef]
34. Tong, B.; Li, Z.; Wang, G.; Zhang, W. How wireless power charging technology affects sensor network deployment and routing. In Proceedings of the 2010 IEEE 30th International Conference on Distributed Computing Systems, Genoa, Italy, 21–25 June 2010; pp. 438–447.
35. Shi, L.; Han, J.; Han, D.; Ding, X.; Wei, Z. The dynamic routing algorithm for renewable wireless sensor networks with wireless power transfer. *Comput. Netw.* **2014**, *74*, 34–52. [CrossRef]
36. Cetinkaya, O.; Dinc, E.; Koca, C.; Merrett, G.V.; Akan, O.B.; Energy-neutral wireless-powered networks. *IEEE Wirel. Commun. Lett.* **2019**. [CrossRef]
37. Park, J.J.; Moon, J.H.; Lee, K.Y.; Kim, D.I. Adaptive mode switching algorithm for dual mode SWIPT with duty cycle operation. In Proceedings of the 2018 IEEE 19th International Workshop on Signal Processing Advances in Wireless Communications (SPAWC), Kalamata, Greece, 25–28 June 2018.
38. Setiawan, D.; Aziz, A.A.; Kim, D.I.; Choi, K.W. Experiment, modeling, and analysis of wireless-powered sensor network for energy neutral power management. *IEEE Syst. J.* **2017**, *12*, 3381–3392. [CrossRef]
39. Choi, K.W.; Ginting, L.; Rosyady, P.A.; Aziz, A.A.; Kim, D.I. Wireless-powered sensor networks: How to realize. *IEEE Trans. Wirel. Commun.* **2016**, *16*, 221–234. [CrossRef]
40. Long, T.; Ozger, M.; Cetinkaya, O.; Akan, O.B. Energy neutral internet of drones. *IEEE Commun. Mag.* **2018**, *56*, 22–28. [CrossRef]
41. Singh, S.K.; Kumar, P.; Singh, J.P. A survey on successors of LEACH protocol. *IEEE Access* **2017**, *5*, 4298–4328. [CrossRef]
42. Yang, Z.; Xu, W.; Pan, Y.; Pan, C.; Chen, M. Optimal fairness-aware time and power allocation in wireless powered communication networks. *IEEE Trans. Commun.* **2018**, *66*, 3122–3135. [CrossRef]
43. Heinzelman, W.R.; Chandrakasan, A.; Balakrishnan, H. Energy-efficient communication protocol for wireless microsensor networks. In Proceedings of the 33rd annual Hawaii international conference on system sciences, Maui, HI, USA, 4–7 January 2000; p. 10.
44. Choi, H.H.; Lee, J.R. Distributed transmit power control for maximizing end-to-end throughput in wireless multi-hop networks. *Wirel. Pers. Commun.* **2014**, *74*, 1033–1044. [CrossRef]
45. Sasikumar, P.; Khara, S. K-means clustering in wireless sensor networks. In Proceedings of the 2012 Fourth International Conference on Computational Intelligence and Communication Networks, Mathura, India, 3–5 November 2012; pp. 140–144.
46. Choi, H.H.; Shin, W. Slotted ALOHA for wireless powered communication networks. *IEEE Access* **2018**, *6*, 53342–53355. [CrossRef]

47. Izadi, D.; Abawajy, J.; Ghanavati, S.; Herawan, T. A data fusion method in wireless sensor networks. *Sensors* **2015**, *15*, 2964–2979. [CrossRef]
48. Yang, Z.; Xu, W.; Pan, Y.; Pan, C.; Chen, M. Energy efficient resource allocation in machine-to-machine communications with multiple access and energy harvesting for IoT. *IEEE Internet Things J.* **2018**, *5*, 229–245. [CrossRef]